Available online at www.sciencedirect.com
SCIENCE DIRECT
Biochimica et Biophysica Acta 1715 (2005) 1 – 5
BIOCHIMICA ET BIOPHYSICA ACTA
BBA
http://www.elsevier.com/locate/bba

Rapid report

Shape relaxations in a fluid supported membrane during hydrolysis by phospholipase A_2

Uffe Bernchou Jensen, Adam Cohen Simonsen*

MEMPHYS Center for Biomembrane Physics, Physics Department, University of Southern Denmark, Campusvej 55, DK-5230 Odense M, Denmark

Received 24 May 2005; received in revised form 12 July 2005; accepted 12 July 2005
Available online 25 July 2005

Abstract

The behavior of a fluid supported membrane during hydrolysis by phospholipase A_2 is for the first time visualized by time-resolved fluorescence imaging. After a lag phase, hydrolysis proceeds from the boundary of existing holes and via nucleation of new holes. During subsequent hydrolysis, the shape of the membrane boundary is determined both by hydrolysis and by shape relaxations due to the action of line tension. This is manifested by the appearance of Rayleigh instabilities in membrane rims and by an effect analogous to domain coarsening in phase transitions in which membrane holes decay when they are within a certain distance from larger and expanding holes.

Keywords: Phospholipase A_2; Fluid supported membrane; Fluorescence microscopy; Line tension

The degradation and modification of biomembranes by the action of lipases are important but still incompletely understood phenomena. Particular attention has been paid to phospholipase A_2 (PLA_2) catalyzing the hydrolysis of phospholipids at the sn-2 ester bond to yield lysophospholipids (lysoPC) and fatty acids (FA). PLA_2 is interfacially activated [1] meaning that it has a higher activity towards interfacially organized lipids (e.g., membranes or monolayers) than towards free lipids. Moreover, the detailed molecular organization of the lipid interface as determined by the thermodynamic state of the membrane as well as non-equilibrium defect structures are critical factors influencing PLA2 activity [2,3].

For example, fluorescence imaging has shown [4] that the fluid part of membranes that exhibit solid–liquid coexistence is hydrolyzed faster than the solid domains. This study also indicated that on a free-standing and intact vesicle, PLA_2 adsorbs uniformly over the area of the fluid phase domains. Contrary to this, it is known from AFM imaging that supported membranes in the solid state [5–7] are hydrolyzed from the perimeter of existing holes and by nucleation of new holes in the membrane surface. Recent AFM data [8] have shown that the hydrolysis of ripple phase membranes has distinct features associated with the corrugated morphology of these membranes.

Although detailed imaging of solid-phase membranes has been achieved during hydrolysis, little is known about the dynamic response of a fluid supported membrane during hydrolysis. We expect this more biologically relevant system to exhibit a fundamentally different dynamics because the fluidity allows the membrane to respond dynamically to morphological changes induced by the hydrolysis. In particular, if membrane holes are formed during hydrolysis, the line tension which acts as a contractive force along the perimeter of holes should manifest itself in relaxations of the hole shapes which is made possible due to the fluid nature of the membrane. We have recently developed a procedure based on spincoating [9] to prepare supported bilayers of general composition. This procedure allows fluid supported membranes to be prepared also at physiological salt concentrations and we have for the first time visualized the complete PLA_2 catalyzed hydrolysis of these substrates by time-resolved fluorescence imaging.

1-Palmitoyl-2-oleoyl-*sn*-glycero-3-phosphocholine (POPC) was purchased from Avanti Polar Lipids and 1,1′-diocta-

* Corresponding author.
E-mail address: adam@memphys.sdu.dk (A.C. Simonsen).

0005-2736/$ - see front matter © 2005 Elsevier B.V. All rights reserved.
doi:10.1016/j.bbamem.2005.07.002

decyl-3,3,3′,3′-tetramethylindocarbocyanine perchlorate ($DiIC_{18}$) from Molecular Probes. Solvents (hexane, methanol) were all HPLC grade quality and MilliQ water was used throughout. Snake venom PLA_2 from *Agkistrodon piscivorus piscivorus* was a gift from R. L. Biltonen, University of Virginia. HEPES buffer (10 mM HEPES (pH = 8.0), 150 mM NaCl, 30 μM $CaCl_2$ and 10 μM EDTA) was used for membrane hydration and for suspension of PLA_2. Freshly cleaved muscovite mica (Plano GmbH, Germany) with a size of 8×8 mm^2 was used for all coating experiments and the preparation of supported POPC membranes by spincoating was done as described previously [9] with lipid containing 0.7% DiI-C_{18}. Briefly, the spincoating method consists of placing a 20-μl droplet of POPC in a hexane/methanol (97:3) solution onto the mica support and immediately thereafter spinning the sample to 3000 rpm for 40 s while the solvent evaporates. A Chemat Technology, KW-4A spincoater was used for the coating process. After overnight storage under vacuum, the sample was hydrated in HEPES buffer and annealed to 80 °C for 3 h to yield a single and highly uniform supported membrane. Excess lipid was removed by washing with buffer while at 80 °C and the success of the washing was monitored continuously. Epi-fluorescence microscopy of the supported membrane was performed with the sample placed in a microscope chamber (Lab-tek Brand Products, Naperville IL) on a Nikon TE2000 inverted microscope and using a 40× long working distance (ELWD) objective. Fluorescence excitation was done with a halogen lamp and using a G-2A filtercube (Nikon). During hydrolysis, fluorescence images were recorded at 10 s intervals with a high sensitivity CCD camera (Sensicam em, PCO-imaging, Kelheim, Germany).

The fluorescence images acquired during hydrolysis show the distribution of DiI-C_{18} on the surface. This probe is chemically different from a phospholipid and is not hydrolyzed by the enzyme. Fig. 1A shows the appearance of a region (211×211 μm^2) of the membrane initially containing holes that cover 4% of the membrane surface. We have deliberately included a minute fraction of pre-existing holes to be able to compare the hydrolysis in these regions with the response from uniform membrane regions. These pre-formed holes are formed during the washing procedure as described above and they are stable over time until the addition of the enzyme. They are often non-circular which indicates that the boundary is pinned to the support. This is unlike holes formed by hydrolysis that can relax to circular shapes. Except for the localized holes, the initial membrane is completely uniform and the probe is uniformly distributed. Separate AFM studies on spincoated supported POPC membranes [9] have confirmed that the substrates are uniform and without holes also on the nanometer scale. The time sequence in Fig. 1A–H shows the hydrolysis of the membrane after the chamber is flushed with PLA_2 (200 nM) at time $t = 0$ s. It is well known that hydrolysis of bilayers by PLA_2 to varying degree exhibits a lag-burst phenomenon by which hydrolysis changes from an initially low to high activity [1,2,6]. We observe a lag-phase of 1500–1800 s after which hydrolysis proceeds as visualized by the generation of dark regions that are depleted in probe. The

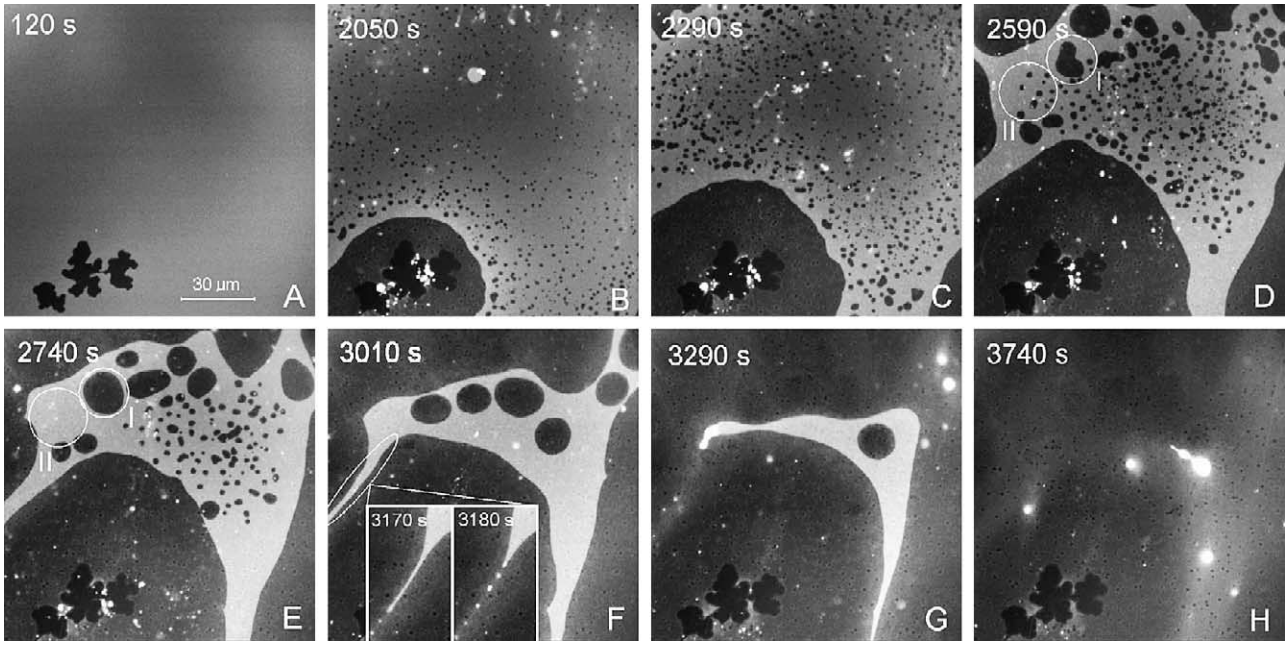

Fig. 1. Time resolved fluorescence imaging of a fluid supported POPC membrane at progressive stages of hydrolysis by phospholipase A_2 (200 nM, added at $t = 0$). Images of a fixed area were recorded in 10-s intervals and only representative images are shown. Initially, the membrane displays uniform fluorescence except for the holes in the lower left corner of image field. After a lag phase, a burst in hydrolysis occurs, both from the existing holes and by nucleation of small holes over the entire membrane area. Regions I and II (D, E) and the inserts in (F) are further explained in the text.

reaction products are to some extent soluble in the buffer [6], but it is also known from recent and similar experiments on SiO_2 [10] that a substantial fraction of the bilayer material can remain on the support after hydrolysis. This is in line with our observation that a fraction of the probe remains on the surface after the reaction. Another fraction of the probe goes to the unreacted part of the bilayer and gives rise to an increase in fluorescence intensity near the perimeter of the unreacted membrane (most clearly in Fig. 1B).

Overall, the onset of membrane hydrolysis occurs by two distinct mechanisms: one is the rapid expansion of holes from the perimeter of the existing holes after the lag phase. Another mechanism is a rather uniform nucleation of many small holes over the entire membrane area. The two mechanisms are, however, not independent: nucleation of the small holes occurs first and is initiated from the perimeter of the existing holes, whereafter small holes are formed gradually over the entire membrane area in a period of 2–3 min. Following this process, rapid hydrolysis takes place from the perimeter of the preformed holes and at a lower rate at the nucleated holes.

The membrane morphology during the subsequent hydrolysis (Fig. 1B–H) is set as an intricate inter-play between hydrolysis from the available perimeter and relaxations in hole shapes from minimization of line tension energy. The fluidity of the membrane allows line tension to have a dynamic effect on membrane morphology which therefore exhibits a dynamic behavior which is very different from what is observed in solid membranes. Line tension seeks to minimize the total perimeter for a given membrane area and there are many ways this can be observed: For example, non-circular holes become circular and that small holes disappear while larger holes grow. The basic mechanism behind this last phenomenon is that when a number of small holes area transformed into a larger hole with the same area, the overall hole perimeter decreases and the process is therefore energetically favorable. Another specific observation demonstrating both the fluidity and the action of line tension is the appearance of Rayleigh instabilities [11] in membrane rims. Fig. 1F (inserts) shows a thin rim of membrane formed by hydrolysis and decaying into droplets between to consecutive frames. The decay is energetically favored when at a certain area, the perimeter of a series of droplets is comparable to the perimeter of the rim. As another illustration of these effects consider the evolution of the encased regions denoted I and II in Fig. 1D and E. Between these two frames ($\Delta t = 150$ s), the small holes within region I are closed while the larger hole in region II is expanded. Contributing to the expansion of the larger hole is both the hydrolysis of membrane from the perimeter of the hole and merging of smaller neighboring holes with the large hole. The disappearance of small holes appears to be closely related to their proximity to larger holes that are expanding.

This observation is more evident if we analyze the image sequence in terms of the intensity difference between image frames. Fig. 2 shows images that are generated by subtracting the pixel intensity between two images spaced at 30-s intervals. In this representation, areas in which the pixel intensity has decreased are dark, whereas regions of increasing pixel intensity are bright. The uniform gray background level represents an intensity difference close to zero. Shortly after the onset of hydrolysis, Fig. 2A shows the rapid expansion of the largest hole and the simultaneous closing of small holes within a critical distance of $\delta \sim 5$ μm from the perimeter of the larger hole. Note that the situation in Fig. 2A is quasi-stationary, meaning that the distance δ and the rate of expansion of the large hole are constant over a period of 400 s. At a more progressed stage of hydrolysis, Fig. 2B shows how larger holes (highlighted) are shrinking only in those regions that are within a critical distance of ~10 μm from the perimeter of the membrane patch. One possible interpretation of these observations is that enzymes are recruited to the perimeter of the larger holes and at the same time depleted from the perimeter of the smaller holes. This may occur by diffusive lateral transport in the

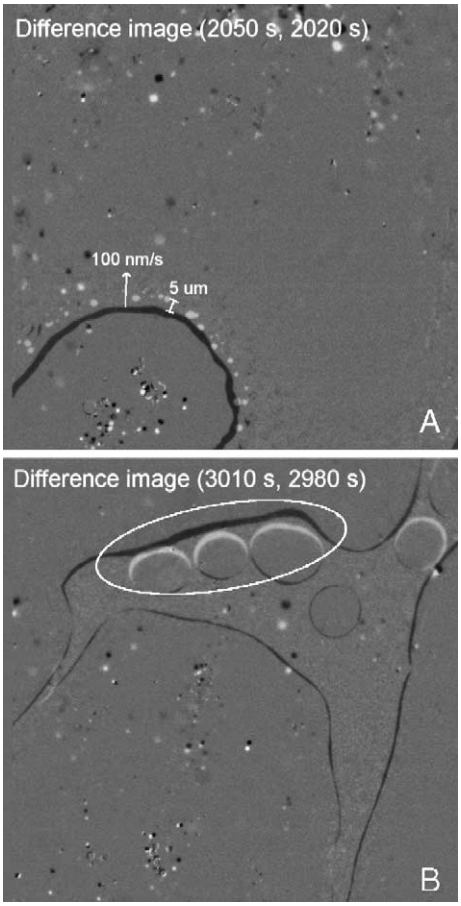

Fig. 2. Difference-images generated by subtraction of the image at shorter time from an image taken at a later time (time values indicated). The gray background level represents a pixel difference close to zero. Dark regions represent a negative difference corresponding to loss of fluorescent area while bright areas represent an increase in area. Examples are shown for times shortly after the lag phase (A) and for intermediate times (B).

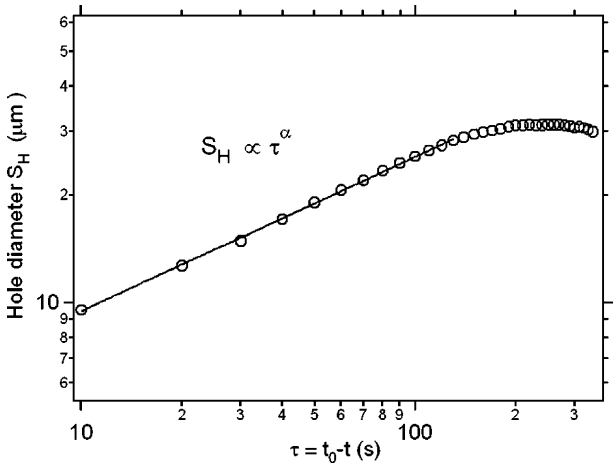

Fig. 3. Typical time evolution of the hole diameter S_H before collapse (increasing time corresponds to decreasing τ). Initially, the hole increases due to hydrolysis and fusion with other holes. Later, the hole decay is described by a power law with an average exponent $\alpha = 0.27 \pm 0.14$.

membrane plane from the smaller to the larger holes, but it may also be combined with an exchange of enzymes in the aqueous phase. Since we cannot separate these two mechanisms, it is not feasible to derive a quantitative measure for the enzyme transport based on the fluorescence images alone.

The dynamics described above is suggestive of a mechanism for hole formation and closure analogous to Ostwald ripening observed in crystal growth. In crystal growth, Ostwald-ripening [12,13] describes the common observation that, after nucleation of crystallites, large crystals are growing at the expense of smaller ones because the system seeks to minimize of the overall interface-free energy. Under certain conditions, the decay of aggregates is described by a power law in which the size $S_A \propto (t_0 - t)^{\alpha}$ and t_0 is the decay time of the aggregate. The exponent α is 1/3 when the coarsening dynamics is diffusion limited and 1/2 in case of an interface limited dynamics [14,15]. Domain coarsening has been observed in coexisting liquid phases of phospholipid/cholesterol monolayer films [16] which is a fluid 2-dimensional system similar to the present. This system was shown to exhibit a coarsening dynamics with an exponent of $\alpha = 0.28 \pm 0.01$ close to the diffusion-limited theoretical prediction. The present observations regarding decay of membrane holes have some striking similarities with domain coarsening in 2-dimensional systems. However, the coarsening of hole sizes is now superimposed on the hydrolysis kinetics occurring at the hole boundaries which makes the total dynamics of hole shapes highly complex.

To quantify these considerations, we have taken individual holes in the times series and analyzed the time evolution of the decay process. Fig. 3 shows in a log–log plot the typical time evolution close to disappearance of a hole. For consistency, the hole diameter S_H is computed as the diameter of a circle with the same area as the hole. Initially, the hole increases by hydrolysis while at later times, line tension takes over and leads to collapse of the hole. The collapse regime occurs over roughly one order of magnitude in time and is approximated by a power law $S_H \propto (t_0 - t)^{\alpha}$. The average value for the exponent (11 holes) is $\alpha = 0.27 \pm 0.14$, but with values in the range 0.14–0.45. This indicates a quantitative link between the observed hole dynamics and previous results regarding domain coarsening in lipid monolayer films. However, the large variation among the measured exponent values warrants some caution against a stronger conclusion since we also know that the hole dynamics is determined both by line tension and hydrolysis.

By using a procedure to count and subtract the number of bright pixels from the number of dark pixels in each difference-image (as shown in Fig. 2), we are able to obtain the net decrease in fluorescent membrane area at each time step. In this way, we can construct the time evolution of the net membrane area and the rate of change of area (dA/dt) for the sequence, as shown in Fig. 4. The system clearly exhibits lag-burst kinetics as seen from the sudden increase in the rate of hydrolysis at around $t = 1800$ s. This lag time (region I) is variable among similar preparations, but comparable to what has been found previously for supported DPPC membranes [6]. The rate of decrease of membrane area (dA/dt) after the lag phase undergoes different characteristic stages, as evident from Fig. 4. After the sudden increase in the burst region (II, 300 s), (dA/dt) is relatively constant over a period of ~800 s (III) until it decreases in a linear way (IV) to zero. This behavior bears a strong resemblance to the time evolution of the membrane perimeter L as measured on DPPC membranes by AFM [6] and indicating a relation of the type:

$$\frac{dA}{dt} \propto -L \tag{1}$$

Where L is the total perimeter for a given field of view and dA/dt is the corresponding rate of area change in the same window. Under this assumption, the constant rate of

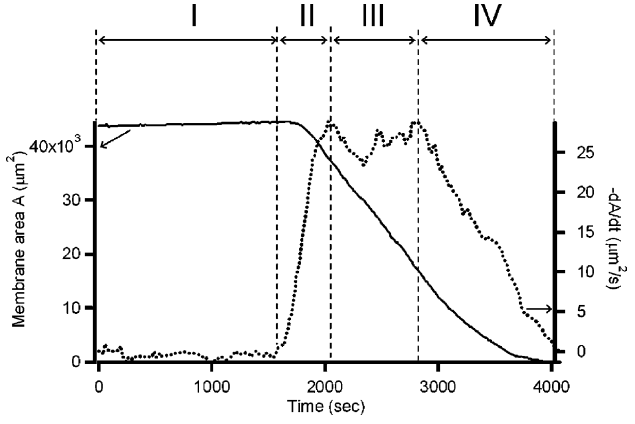

Fig. 4. The time evolution of the total membrane area (line) and the rate of area decrease (dots) derived by analysis of images in Fig. 1. Four distinct time intervals (I–IV) of the hydrolysis are indicated and discussed further in the text.

hydrolysis in region (III) is explained by the fact that the perimeter available for enzyme attack in this period remains rather constant. The linear decrease of dA/dt in region (IV) can be understood if we assume that in this region, the perimeter is related to the area as $L \propto \sqrt{A}$. This would be the case for a circular membrane patch, but may also hold approximately for more complex boundary shapes. Assuming this relationship, Eq. (1) is easily solved and will indeed exhibit a linear decrease in dA/dt with respect to time.

In summary, we have visualized that a fluid supported membrane when hydrolyzed by PLA_2 undergoes relaxations in the boundary shape resulting from the fluidity of the membrane and the action of line tension. After a lag phase, a burst in hydrolysis occurs starting from existing holes and by nucleation of new holes. During hydrolysis, a coarsening of hole sizes is observed in which smaller holes decay when they are within a certain critical distance from a larger and expanding hole. This effect resembles Ostwald ripening in crystal growth and can quantitatively be described by a power law with an average exponent that is close to the diffusion-limited prediction. A related effect is the appearance of Rayleigh instabilities in membrane rims that have shrunk below a critical width. We have quantified the rate of area change (dA/dt) which grows rapidly to a constant value and then decreases linearly to zero. This is in line with the interpretation that hydrolysis occurs at the boundary at a rate proportional to the boundary length.

Acknowledgements

We thank Chad Leidy, Per Lyngs Hansen and Ole G. Mouritsen (MEMPHYS) for helpful discussions.

We also thank the following sources for financial support: The Danish National Research Foundation for support via a grant to MEMPHYS-Center for Biomembrane Physics. The Augustinus Foundation. The Oticon Foundation. The European Commission under contract NMP4-CT-2003-505211 (BIOSCOPE).

References

[1] R. Verger, M.C.E. Mieras, G.H. de Haas, Action of phospholipase A_2 at interfaces, J. Biol. Chem. 248 (1973) 4023–4034.
[2] W.R. Burack, R.L. Biltonen, Lipid bilayer heterogeneities and modulation of bilayer activity, Chem. Phys. Lipids 73 (1994) 209–222.
[3] T. Hønger, K. Jørgensen, D. Stokes, R.L. Biltonen, O.G. Mouritsen, Phospholipase A_2 activity and physical properties of lipid-bilayer substrates, Methods Enzymol. 286 (1997) 168–190.
[4] S.A. Sanchez, L.A. Bagatolli, E. Gratton, T.L. Hazlett, A two-photon view of an enzyme at work: *Crotalus atrox* venom PLA(2) interaction with single-lipid and mixed-lipid giant unilamellar vesicles, Biophys. J. 82 (2002) 2232–2243.
[5] M. Grandbois, H. Clausen-Schaumann, H.E. Gaub, Atomic force microscope imaging of phospholipid bilayer degradation by phospholipase A_2, Biophys. J. 74 (1998) 2398–2404.
[6] L.K. Nielsen, J. Risbo, T.H. Callisen, T. Bjørnholm, Lag-burst kinetics in phospholipase A_2 hydrolysis of DPPC bilayers visualized by atomic force microscopy, Biochim. Biophys. Acta Biomembr. 1420 (1999) 266–271.
[7] K. Balashev, M. Gudmand, L. Iversen, T.H. Callisen, A. Svendsen, T. Bjørnholm, *Humicola lanuginosa* lipase hydrolysis of monooleoyl-rac-glycerol at the lipid–water interface observed by atomic force microscopy, Biochim. Biophys. Acta Biomembr. 1615 (2003) 93–102.
[8] C. Leidy, O.G. Mouritsen, K. Jorgensen, G.H. Peters, Evolution of a rippled membrane during phospholipase A_2 hydrolysis studied by time-resolved afm, Biophys. J. 87 (2004) 408–418.
[9] A.C. Simonsen, L.A. Bagatolli, Structure of spin-coated lipid films and domain formation in supported membranes formed by hydration, Langmuir 20 (2004) 9720–9728.
[10] H.P. Vacklin, F. Tiberg, G. Fragneto, R.K. Thomas, Phospholipase A_2 hydrolysis of supported phospholipid bilayers: a neutron reflectivity and ellipsornetry study, Biochemistry 44 (2005) 2811–2821.
[11] Lord Rayleigh, On the instability of jets, Proc. Lond. Math. Soc. 10 (1878) 4–13.
[12] J.D. Gunton, M.S. Miguel, P.S. Sahni, The Dynamics of First Order Phase Transitions, Academic Press, London, 1983.
[13] M. Zinke-Allmang, Phase separation on solid surfaces: nucleation, coarsening and coalescence kinetics, Thin Solid Films 346 (1999) 1–68.
[14] O.G. Mouritsen, Pattern formation in condensed matter, Int. J. Mod. Phys. B 4 (1990) 1925–1954.
[15] O.G. Mouritsen, Kinetics of Ordering and Growth in 2-D Systems, Plenum Press, New York, 1990.
[16] M. Seul, N.Y. Morgan, C. Sire, Domain coarsening in a two-dimensional binary mixture: growth dynamics and spatial correlations, Phys. Rev. Lett. 73 (1994) 2284–2287.